Hamiltonian MCMC Based Framework for Time-variant Rare Event Uncertainty Quantification

Konstantinos G. Papakonstantinou
Associate Professor, Department of Civil and Environmental Engineering, The Pennsylvania State University, University Park, USA

Elsayed Eshra
Graduate Student, Department of Civil and Environmental Engineering, The Pennsylvania State University, University Park, USA

Hamed Nikbakht
Data Scientist, Risk Management Solutions Inc., Palo Alto, USA

ABSTRACT: Accurate and efficient rare event uncertainty quantification is of ever-increasing significance, including for natural hazard cases characterized by substantial dynamic loads. In this work, our computationally efficient framework for precisely estimating rare events probabilities, termed *Approximate Sampling Target with Post-processing Adjustment* (ASTPA), is further examined and demonstrated to maintain its effectiveness and applicability even on complex first-passage dynamic problems. The ASTPA framework weighs the multi-dimensional random variable space by a cumulative distribution function that utilizes the limit-state expression, to construct an approximate sampling target distribution. While any appropriate sampling scheme can be used to sample this constructed target distribution, Hamiltonian Markov Chain Monte Carlo (HMCMC) samplers have shown notable efficiency in this task, particularly our developed *Quasi-Newton mass preconditioned Hamiltonian MCMC* (QNp-HMCMC) approach. Given that the acquired samples are drawn from an approximate target, a post-processing adjustment is performed through a devised original *inverse importance sampling* (IIS) procedure. The capabilities and efficiency of the discussed approach are demonstrated and compared against the Subset Simulation method in a series of high-dimensional, non-linear, stochastic dynamic problems.

1. INTRODUCION

In this work, we investigate the application of our developed Hamiltonian MCMC-based framework for estimating first-passage probabilities of complex dynamic systems. These systems are often described by high-dimensional random variable spaces, due to the system's inherent uncertainties and the random variables involved in simulating the dynamic excitations as stochastic processes. Despite many advances in the field of computational reliability analysis, efficient first-passage probabilities estimation remains a significant challenge (Andrieu-Renaud et al., 2004;

Song and Der Kiureghian, 2006; Zhang et al., 2017). As a step towards universally addressing this challenge, we employ our computationally efficient framework, termed *Approximate Sampling Target with Post-processing Adjustment* (ASTPA), which has demonstrated exceptional performance in general static problems, including challenging cases of high-dimensionality, multi-modality, non-Gaussianity, and very small probabilities (Papakonstantinou et al., 2022, 2023).

The ASTPA framework, as its name suggests, consists of two main stages: *(i)* constructing and acquiring samples from the approximate sampling

target, and *(ii)* performing a post-processing adjustment to compute the unbiased target probability. The approximate sampling target, generally constructed utilizing a cumulative distribution function and the limit-state expression, successfully places greater importance on the relevant regions of interest in the random variable space and manages to accordingly guide the related samples. Hamiltonian Markov Chain Monte Carlo (HMCMC) samplers, particularly our developed Quasi-Newton mass preconditioned Hamiltonian MCMC (QNp-HMCMC) approach, have shown notable efficiency in sampling this constructed target distribution. After acquiring the samples, the approximate sampling target must be appropriately normalized to correctly compute the target probability. This is achieved through the post-processing adjustment step using a novel *inverse importance sampling* (IIS) procedure, that utilizes an importance sampling density properly suggested based on the already acquired HMCMC samples.

The focus of this work is on further utilizing the ASTPA framework in estimating first-passage probabilities of complex dynamic problems, described in both Gaussian and non-Gaussian stochastic spaces. The ASTPA framework's ability to directly work on non-Gaussian spaces is advantageous in scenarios where the transformation to the favorable and preferred Gaussian space cannot be achieved. Finally, the capabilities and efficiency of the discussed framework are demonstrated and compared against the Subset Simulation method (Au and Beck, 2001) in a series of high-dimensional, nonlinear, stochastic dynamic problems, involving model uncertainties and stochastic processes expressed through white noise, Karhunen-Loève (K-L) expansion, and the Spectral Representation Method.

2. FIRST-PASSAGE PROBABILITIES

The first-passage probability is defined by the probability that the interested response of a stochastic dynamic system, $Z(t, \boldsymbol{\theta})$, reaches or exceeds a prescribed threshold, λ, for the first time within a given time interval $[0, T]$. The first-passage probability P_F is hence expressed as:

$$P_F = \Pr\{Z(t, \boldsymbol{\theta}) \geq \lambda, \exists t \in [0, T]\} \quad (1)$$

where Pr is the probability operator; $\boldsymbol{\theta}$ is a time-independent random parameter vector $[\theta_1, ..., \theta_d]^T$, describing the dynamic system; $F \subset \mathbb{R}^d$ is the targeted rare event in the parameter space. Since the occurrence of the rare event is indicated by any attainment or surpassing of the prescribed threshold λ, the first-passage probability can be rewritten as:

$$P_F = \Pr\{\max_t Z(t, \boldsymbol{\theta}) \geq \lambda, \exists t \in [0, T]\} \quad (2)$$

The system performance is thus typically described using a limit state function $g(t, \boldsymbol{\theta})$, defined as:

$$g(t, \boldsymbol{\theta}) = \lambda - Z(t, \boldsymbol{\theta}) \quad (3)$$

Eq. (2) can be then accordingly expressed as:

$$P_F = \Pr\{\min_t g(t, \boldsymbol{\theta}) \leq 0, \exists t \in [0, T]\}$$
$$= \Pr\{G \leq 0\} \quad (4)$$

where $G = \min_{t \in [0, T]}\{g(t, \boldsymbol{\theta})\}$. Therefore, the first-passage probability can be computed as a *d*-fold integral, as:

$$P_F = \mathbb{E}_{\pi_\Theta}[I_F(\boldsymbol{\theta})] = \int_{G \leq 0} I_F(\boldsymbol{\theta}) \pi_\Theta(\boldsymbol{\theta}) d\boldsymbol{\theta} \quad (5)$$

where $I(.)$ is the indicator function with: $I_F(\boldsymbol{\theta}) = 1$ if $\boldsymbol{\theta} \in G \leq 0$ and $I_F(\boldsymbol{\theta}) = 0$ otherwise; $\mathbb{E}$ is the expectation operator, and π_Θ is the joint probability density function (PDF) for Θ.

In rare events, the first-passage probabilities are typically very small, e.g., in order of $P_F \sim 10^{-4} - 10^{-9}$. Given that complex engineering systems are often described by high-dimensional random variable spaces, and are computationally expensive, using direct Monte Carlo approaches to evaluate such probabilities through the described integration in Eq. (5) is generally infeasible, due to the prohibitive number of required system evaluations (model calls), and the associated high coefficient of variation (C.o.V).

Importance sampling (IS) is a well-known, computationally efficient, variance-reduction approach capable of computing such integrals. The IS approach involves sampling from an alternative sampling density, referred to as the importance sampling density (ISD), $h(\boldsymbol{\theta})$, that places greater importance on regions of interest in the random variable space. This results in an increased number of

samples being drawn from these regions, thereby reducing the number of required model calls. The IS estimate of Eq. (5) is formulated as:

$$
\begin{aligned}
P_F &= \int_{G \leq 0} I_F(\boldsymbol{\theta}) \frac{\pi_\Theta(\boldsymbol{\theta})}{h(\boldsymbol{\theta})} h(\boldsymbol{\theta}) d\boldsymbol{\theta} \\
&= \mathbb{E}_{h(\boldsymbol{\theta})}[I_F(\boldsymbol{\theta}) \frac{\pi_\Theta(\boldsymbol{\theta})}{h(\boldsymbol{\theta})}]
\end{aligned}
\tag{6}
$$

A theoretically optimal ISD can be given by (Biondini, 2015):

$$
\hat{h}(\boldsymbol{\theta}) = \frac{1}{P_F}(I_F(\boldsymbol{\theta}) \times \pi_\Theta(\boldsymbol{\theta}))
\tag{7}
$$

Yet, it is evident that this ISD cannot be utilized due to the fact that the normalizing constant in Eq. (7) is the sought target probability P_F. The discontinuity and non-smoothness of the indicator function also impose significant sampling challenges, particularly in cases of high dimensionality and/or multimodality. As a near optimal ISD is generally considered beneficial, numerous methods have been proposed for approximating the theoretically optimal ISD, such as (Papaioannou et al., 2019). The ASTPA framework, however, offers an alternative approach by directly constructing an unnormalized sampling target in a distinct context, as discussed in subsequent sections.

3. APROXIMATE SAMPLING TARGET WITH POST-PROCESSING ADJUSTMENT (ASTPA)

The proposed ASTPA framework consists of two main stages. The first stage involves constructing and sampling an approximate sampling target, followed by a post-processing adjustment step to compute an unbiased target probability.

3.1. Approximate Sampling Target

In accordance with the previous discussion on the optimal ISD, we analyze here our approach to construct an unnormalized sampling target. It should be noted that after acquiring the samples, this sampling target is appropriately normalized, to correctly compute the target probability. The main idea of our approach is to replace the indicator function in Eq. (7) with a one-dimensional likelihood

function ℓ_{g_θ}, using the limit-state expression $g(\boldsymbol{\theta})$; t is dropped here for generalization purposes. This smoothening of the indicator function has already been suggested and explored in the literature (Papaioannou et al., 2019), albeit in a completely different context. The likelihood function is then expressed here as a logistic CDF, F_{cdf}, with mean $= \mu_{g(\boldsymbol{\theta})}$ and a dispersion factor σ:

$$
\begin{aligned}
\ell_{g_\theta} &= F_{cdf}\left(\frac{-g(\boldsymbol{\theta})}{g_c} \,\middle|\, \mu_{g(\boldsymbol{\theta})}, \, \sigma\right) \\
&= \frac{1}{\left(1 + e^{\frac{(\frac{g(\boldsymbol{\theta})}{g_c}) + \mu_{g(\boldsymbol{\theta})}}{(\frac{\sqrt{3}}{\pi})\sigma}}\right)}
\end{aligned}
\tag{8}
$$

where g_c is a scaling constant. The main reason for this general scaling, $g(\boldsymbol{\theta})/g_c$, is in order to conform the likelihood scale with the density of the sampling space.

Removing the normalizing term $(1/P_F)$, and replacing the indicator function with the likelihood function ℓ_{g_θ}, Eq. (7) is then written as:

$$
\tilde{h}(\boldsymbol{\theta}) = \ell_{g_\theta} \times \pi_\Theta(\boldsymbol{\theta})
\tag{9}
$$

where $\tilde{h}(\boldsymbol{\theta})$ represents the approximate sampling target. The suggested likelihood function places greater importance on the rare event domain, i.e., for $\boldsymbol{\theta} \in g(\boldsymbol{\theta}) \leq 0$, similar to the indicator function. In contrast, ℓ_{g_θ} is smooth, continuous, and supported in the entire random variable space, thereby allowing the use of any appropriate sampling technique to sample the constructed sampling target. Having the total number of model calls in mind, as well as the coefficient of variation of the estimator (C.o.V), the suggested value for σ is deemed to be in the range [0.2 0.8]. The mean parameter $\mu_{g(\boldsymbol{\theta})}$ is determined by placing a recommended percentile, $p = 0.1$, of the logistic CDF on the limit-state surface $g(\boldsymbol{\theta}) = 0$ (see (Papakonstantinou et al., 2023) for more details).

3.2. Post-processing Adjustment

To finally compute the first-passage probability, we have to adjust the IS estimate in Eq. (6), to consider the fact that the sampling target $\tilde{h}(\boldsymbol{\theta})$ is unnormalized. Assuming the ISD $h(\boldsymbol{\theta}) = \tilde{h}(\boldsymbol{\theta})/C_h$,
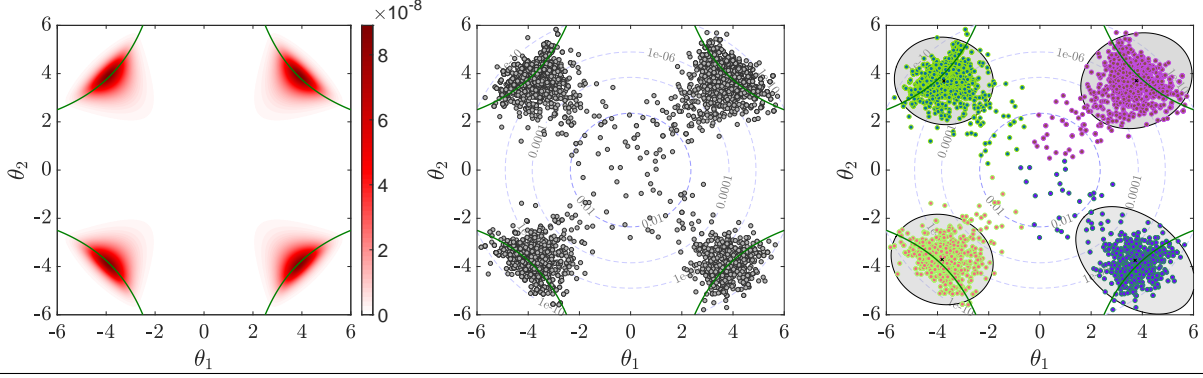
Figure 1: The ASTPA framework is depicted through the above figures. They represent the approximate sampling target, sampled target distribution samples based on our HMCMC-based method, and fitted Gaussian Mixture Model describing the simulated samples, from left to right, respectively.

where C_h is the normalizing constant of the constructed sampling target, Eq. (6) is rewritten as:

$$P_F = \mathbb{E}_{\tilde{h}(\boldsymbol{\theta})}[I_F(\boldsymbol{\theta}) \frac{C_h \pi_\Theta(\boldsymbol{\theta})}{\tilde{h}(\boldsymbol{\theta})}] \qquad (10)$$

Assuming now that N samples have been sampled based on our constructed sampling target $\tilde{h}(\boldsymbol{\theta})$, using any appropriate sampling technique, and substituting $\tilde{h}(\boldsymbol{\theta})$ as defined in Eq. (9), the first-passage probability can be computed as:

$$P_F = \left(\frac{1}{N} \sum_{i=1}^{N} \frac{I_F(\boldsymbol{\theta}_i)}{\ell_{g_{\boldsymbol{\theta}}}(\boldsymbol{\theta}_i)} \right) C_h \qquad (11)$$

To determine the normalizing constant C_h, an original post-sampling step is devised at this stage using our *inverse importance sampling* procedure, i.e., having the samples, choose a pertinent importance sampling density (ISD), $Q(.)$, automatically, based on the samples. Given that, this normalizing constant is then computed as:

$$C_h = \frac{1}{M} \sum_{i=1}^{M} \frac{\tilde{h}(\boldsymbol{\theta}_i)}{Q(\boldsymbol{\theta}_i)} \qquad (12)$$

where $Q(.)$ can be, for example, a computed Gaussian Mixture Model (GMM), based on the already available samples and the generic Expectation-Maximization (EM) algorithm. Since HMCMC samplers are chosen in this work to generate samples from $\tilde{h}(\boldsymbol{\theta})$, these samples will be called HMCMC samples hereafter. Accurate fitting of a GMM allows for the direct utilization of the original HMCMC samples to compute the normalizing constant C_h. However, given that the accuracy of GMMs may often deteriorate, particularly in high-dimensional and challenging multi-modal cases, additional samples from the computed $Q(.)$ can be required, just in order to adequately evaluate the normalizing constant C_h. In this latter, more general case, even a quite approximately fitted GMM with diagonal covariance matrices, particularly appropriate for high-dimensional cases, works effectively.

Figure 1 concisely portrays the ASTPA framework by using a multi-modal target distribution. The green curves represent the isolated regions of the limit-state function $g(\boldsymbol{\theta})$ of this problem, with the rare event domain being outside $g(\boldsymbol{\theta})$, i.e., towards the edges. The left figure displays the constructed approximate sampling target $\tilde{h}(\boldsymbol{\theta})$, which can be visualized in this complex 2D case. The middle figure showcases the samples drawn from the target distribution by our suggested Hamiltonian MCMC variant, as described in the following section. The right figure indicates the GMM, $Q(.)$, fitted based on the HMCMC samples, as discussed above.

4. HAMILTONIAN MARKOV CHAIN MONTE CARLO (HMCMC)

In HMCMC methods, Hamiltonian dynamics are used to produce distant Markov chain samples, thereby avoiding the slow exploration of the state space that results from the diffusive behavior of

4

simple random-walk proposals. Given a parameter of interest $\boldsymbol{\theta}$ with (unnormalized) density $\pi_\Theta(.)$, the HMCMC method introduces an auxiliary momentum variable $\mathbf{z}$ and samples from the joint distribution characterized by $\pi(\boldsymbol{\theta}, \mathbf{z}) \propto \pi_\Theta(\boldsymbol{\theta}) \, \pi_{Z|\Theta}(\mathbf{z}|\boldsymbol{\theta})$, where $\pi_{Z|\Theta}(.|\boldsymbol{\theta})$ is proposed to be a symmetric distribution. With $\pi_\Theta(\boldsymbol{\theta})$ and $\pi_{Z|\Theta}(\mathbf{z}|\boldsymbol{\theta})$ being uniquely described up to normalizing constants, the functions $U(\boldsymbol{\theta}) = -\log \pi_\Theta(\boldsymbol{\theta})$ and $K(\boldsymbol{\theta}, \mathbf{z}) = -\log \pi_{Z|\Theta}(\mathbf{z}|\boldsymbol{\theta})$ are introduced as the potential energy and kinetic energy (Neal, 2011). The total energy $H(\boldsymbol{\theta}, \mathbf{z})$ can be thus expressed as $H(\boldsymbol{\theta}, \mathbf{z}) = U(\boldsymbol{\theta}) + K(\boldsymbol{\theta}, \mathbf{z})$ and is often termed the Hamiltonian H. In most typical cases, the momentum is given by a zero-mean normal distribution (Neal, 2011), $\mathbf{z} \sim \mathbf{N}(0, \mathbf{M})$, and accordingly the kinetic energy can be written as: $K(\boldsymbol{\theta}, \mathbf{z}) = -\log \pi_{Z|\Theta}(\mathbf{z}|\boldsymbol{\theta}) = -\log \pi_Z(\mathbf{z}) = \frac{1}{2}\mathbf{z}^T \mathbf{M}^{-1}\mathbf{z}$, where $\mathbf{M}$ is a symmetric, positive-definite inverse covariance matrix.

HMCMC generates a Metropolis proposal on the joint state-space $(\boldsymbol{\theta}, \mathbf{z})$ by sampling the momentum and simulating trajectories of Hamiltonian dynamics in which the time evolution of the state $(\boldsymbol{\theta}, \mathbf{z})$ is governed by Hamilton's equations, expressed typically by:

$$\frac{d\boldsymbol{\theta}}{dt} = \frac{\partial H}{\partial \mathbf{z}} = \frac{\partial K}{\partial \mathbf{z}} = \mathbf{M}^{-1}\mathbf{z},$$
$$\frac{d\mathbf{z}}{dt} = -\frac{\partial H}{\partial \boldsymbol{\theta}} = -\frac{\partial U}{\partial \boldsymbol{\theta}} = \nabla_\theta \mathscr{L}(\boldsymbol{\theta}) \qquad (13)$$

where $\mathscr{L}(\boldsymbol{\theta})$ denotes the log-density of the target distribution. Given that the analytical solution of the Hamiltonian equations is in general intractable, a symplectic integrator, typically the leapfrog one, can be used to solve them numerically by discretizing time, using some small step size ε, thus simulating solution trajectories of length τ. In connection with the ASTPA framework, it is worth noting that the $\mathscr{L}(\boldsymbol{\theta})$ is the logarithmic form of the approximate sampling target $\tilde{h}(\boldsymbol{\theta})$.

In complex high-dimensional problems, the computational cost of the typical HMCMC sampler may increase considerably and a prohibitive number of model calls may be required. We address this issue here in a developed Newton-type context, where the Hessian matrix, $\mathbf{W}^{-1}$, is approximated without any required additional model calls

per leapfrog step. In the burn-in phase we are still sampling the momentum from an identity mass matrix, $\mathbf{M} = \mathbf{I}$, but the ODEs of Eq. (13) now become:

$$\dot{\boldsymbol{\theta}} = \mathbf{W}\mathbf{M}^{-1}\mathbf{z}, \quad \dot{\mathbf{z}} = \mathbf{W}\nabla_\theta \mathscr{L}(\boldsymbol{\theta}) \qquad (14)$$

This new dynamic scheme efficiently and compatibly provides an approximation of the structure of the target distribution, allowing large informed jumps across the state space. The final estimation of the approximated inverse of the Hessian matrix, $\mathbf{W}$, from the burn-in phase, is then used to define the preconditioned mass matrix, $\mathbf{M} = \mathbf{W}^{-1}$, to sample the momentum in the subsequent phase of the algorithm, where Eq. (13) is again used. For further information on the implementation of the HMCMC samplers within the ASTPA framework, we refer the reader to (Papakonstantinou et al., 2023).

5. NUMERICAL RESULTS

In this section, three stochastic dynamic cases are presented, to indicatively illustrate the efficiency of the proposed approach. Comparisons with Subset Simulation (SuS) results are provided, with a uniform SuS proposal, $\mathbf{U}(-1, 1)$, a number of samples per each subset level, n_s, accordingly defined in each example, and $p_0 = 0.1$, with p_0 being the percentile of the samples that determines the intermediate subsets (Au and Beck, 2001). In all examples, analytical gradients are provided, and the number of limit-state function evaluations for the HMCMC-based methods has been set to roughly provide a C.o.V $\in [0.2, 0.5]$, for comparison purposes. Results for all examples are based on 100 independently performed simulations, to acquire the sample mean and C.o.V. The problem dimension is denoted by d in all cases, and the ASTPA parameters are carefully chosen for all examples here, as also described in (Papakonstantinou et al., 2023), but are not optimized for any of them. The reference first-passage probabilities are estimated by computing the average of 100 independent simulations obtained by SuS with $n_s = 10^5$.

5.1. *Example 1: SDOF Hysteretic Oscillator*

This example studies a SDOF hysteretic oscillator, defined by the following differential equation:

$$m\ddot{x}(t) + c\dot{x} + k[\alpha x(t) + (1 - \alpha)z(t)] = f(t) \quad (15)$$

Table 1: *Performance of various methods on the SDOF oscillator with white noise in example 1(a) ($d = 150$).*

	100 Independent Simulations	SuS	HMCMC	QNp-HMCMC
$\lambda = 0.06$	Number of model calls	8,390	7,507	7,139
$\tau = 0.7$	C.o.V	0.25	0.18	0.18
$\sigma = 0.4$	$\mathbb{E}[\hat{P}_F]$ (Reference $P_F \sim$0.98E-4)	1.02E-4	0.98E-4	0.98E-4
$\lambda = 0.07$	Number of model calls	11,000	8,122	8,183
$\tau = 0.7$	C.o.V	0.37	0.25	0.25
$\sigma = 0.4$	$\mathbb{E}[\hat{P}_F]$ (Reference $P_F \sim$2.35E-6)	2.47E-6	2.37E-6	2.31E-6

Table 2: *Performance of various methods on the SDOF oscillator with K-L expansion in example 1(b) ($d = 200$).*

	100 Independent Simulations	SuS	HMCMC	QNp-HMCMC
$\lambda = 0.18$	Number of model calls	12,800	11,900	12,447
$\tau = 0.7$	C.o.V	0.41	0.40	0.33
$\sigma = 0.5$	$\mathbb{E}[\hat{P}_F]$ (Reference $P_F \sim$3.50E-7)	3.10E-7	3.44E-7	3.53E-7

where $\ddot{x}(t)$, $\dot{x}(t)$, and $x(t)$ are the acceleration, velocity, and displacement of the oscillator at time t, respectively. The $m = 6 \times 10^4\,kg$, $k = 5 \times 10^6\,N/m$, $c = 2m\xi\sqrt{k/m}$, and $\xi = 0.05$ are mass, stiffness, damping coefficient, and damping ratio of the oscillator, respectively. The yielding displacement of the oscillator x_y, and the parameter α are set to $0.04m$ and 0.1, respectively. The hysteretic displacement $z(t)$ follows the Bouc-Wen hysteretic model:

$$\dot{z}(t) = -\gamma|\dot{x}(t)||z(t)|^{\bar{n}-1}z(t) - \beta|z(t)|^{\bar{n}}\dot{x}(t) + A\dot{x}(t) \tag{16}$$

with $\beta = \gamma = \frac{1}{2x_y^{\bar{n}}}$, $\bar{n} = 3$, and $A = 1$. The system is subjected to random input loading $f(t)$, simulated as a stochastic process using two cases: *(i)* Gaussian white noise, and *(ii)* the Karhunen-Loève (K-L) expansion. The details and the results of these two methods are subsequently discussed. The limit-state function is defined in terms of the maximum displacement of the oscillator in the time interval $[0, 10\ sec]$ as:

$$g(t, \boldsymbol{\theta}) = \lambda - \max\left(x(t, \boldsymbol{\theta})\right) \tag{17}$$

5.1.1. *Case 1a: Gaussian white noise*

The random input force is represented as:

$$f(t, \boldsymbol{\theta}) = -m\bar{\sigma}\sum_{i=1}^{d/2}[\theta_i\cos(\omega_i t) + \theta_{\frac{d}{2}+i}\sin(\omega_i t)] \tag{18}$$

where θ_i's, $i = 1, ..., d$, denote independent standard Gaussian random variables; $\omega_i = i\Delta\omega$ is the discrete frequency, and $\Delta\omega = \omega_{cut}/(d/2)$ in which $\omega_{cut} = 15\pi$ is the cut-off frequency; $\bar{\sigma} = \sqrt{(2S\Delta\omega)}$, where $S = 0.005$ is the intensity of the white noise. The number of dimensions is chosen as $d = 150$. In this case, two threshold levels $\lambda = 0.06$ and 0.07 are considered, to evaluate the performance for two distinct first-passage probability levels. The results are presented in Table 1, where the ASTPA parameters are also shown, i.e., the dispersion factor σ and Hamiltonian trajectory length τ. For comparison purposes, the SuS results reported in this example are based on $n_s = 2,000$. It is seen that our HMCMC-based ASTPA framework can outperform the SuS for both probability levels.

5.1.2. *Case 1b: Karhunen-Loève (K-L) expansion*

This second case involves using the Karhunen-Loève (K-L) expansion to simulate $f(t, \boldsymbol{\theta})$ as a zero-mean Gaussian excitation process, represented as:

$$f(t, \boldsymbol{\theta}) = \sum_{i=1}^{d}\theta_i\sqrt{\lambda_i}\phi_i(t) \tag{19}$$

where θ_i's, $i = 1, ..., d$, denote independent standard Gaussian random variables; λ_i, and ϕ_i are the i-th eigenvalue and eigenvector of a Gaussian autocovariance kernel expressed as:

$$C(t_1, t_2) = \exp\left(-(t_1 - t_2)^2/L^2\right) \tag{20}$$

6

Table 3: Performance of various methods on example 2, in the: (a) standard Gaussian space, and (b) non-Gaussian space ($d = 202$).

		100 Independent Simulations	**SuS**	**HMCMC**	**QNp-HMCMC**
(a)	$\lambda = 0.229$ $\tau = 0.7$ $\sigma = 0.6$	Number of model calls	19,264	17,844	16,153
		C.o.V	0.83	0.38	0.35
		$\mathbb{E}[\hat{P}_F]$ (Reference $P_F \sim$2.57E-5)	2.51E-5	2.56E-5	2.51E-5
(b)	$\lambda = 0.229$ $\tau = 1.0$ $\sigma = 0.6$	Number of model calls	–	29,476	24,318
		C.o.V	–	0.48	0.41
		$\mathbb{E}[\hat{P}_F]$ (Reference $P_F \sim$2.57E-5)	–	2.28E-5	2.47E-5

where the correlation length L is set to 0.08. Considering the first 200 terms of the K-L expansion in this application, corresponding to the 200 largest eigenvalues, i.e., $d = 200$, is found to be sufficient. In this case, the threshold λ in Eq. (17) is set to 0.18. The results, accompanied by the ASTPA parameters, are presented in Table 2, and it is shown again that the HMCMC-based ASTPA framework can outperform the SuS method.

5.2. *Example 2: Two-story Shear Frame Structure Under Stochastic Ground Motion*

A two-story nonlinear shear frame structure with uncertain stiffness properties under stochastic ground motion is investigated in this example. The equation of motion of this structure reads:

$$\mathbf{M}\ddot{\mathbf{x}}(t) + \mathbf{C}\dot{\mathbf{x}}(t) + \mathbf{K}[\boldsymbol{\alpha}\mathbf{x}(t) + (1-\boldsymbol{\alpha})\mathbf{z}(t)] = -\mathbf{M}\ddot{X}_g$$

(21)

where $\ddot{\mathbf{x}}$, $\dot{\mathbf{x}}$, and $\mathbf{x}$ are the lateral acceleration, velocity, and displacement vectors of the structure; $\mathbf{M}$, $\mathbf{C}$, and $\mathbf{K}$ are the mass, damping, and stiffness matrices, repectively. The lumped masses and damping coefficients are set to $m = 0.4 \times 10^3\,kg$ and $c = 0.28 \times 10^3 N.s/m$ for both stories, respectively. The stiffnesses of the two stories are considered random normal variables with a mean of $49 \times 10^3 N/m$, and a coefficient of variation of 0.1. It is assumed that only the first story of the frame exhibits hysteretic/nonlinear behavior, with $\boldsymbol{\alpha} = [0,1]^T$. This nonlinear behavior is again modeled using the Bouc-Wen law in Eq. (16), with $\beta = 1$, $\gamma = \bar{n} = 2$, and $A = 1$. The ground motion acceleration is described in the frequency domain by a filtered Kanai-Tajimi power spectral density (PSD),

defined as:

$$S_{\ddot{X}_g}(\omega) = S_0 \frac{\omega_f^4 + 4\xi_f^2\omega_f^2\omega^2}{(\omega_f^2 - \omega^2)^2 + 4\xi_f^2\omega_f^2\omega^2}$$
$$\cdot \frac{\omega^4}{(\omega_s^2 - \omega^2)^2 + 4\xi_s^2\omega_s^2\omega^2}$$

(22)

where $S_0 = 0.01\,m^2/s^3$, $\omega_f = 15\,rad/sec$, $\xi_f = 0.6$, $\omega_s = 1.5\,rad/sec$, and $\xi_s = 0.6$ are the PSD parameters. The ground motion acceleration $\ddot{X}_g$ is simulated based on the PSD in Eq. (22) using the Spectral Representation Method as:

$$\ddot{X}_g(\boldsymbol{\theta}, t) = \sqrt{2}\sum_{i=0}^{\bar{d}-1}\sqrt{S_{\ddot{X}_g}(\omega_i)\Delta\omega}\cos(\omega_i t + \theta_i)$$

(23)

where θ_i's, $i = 1, ..., \bar{d} = 200$, are independent random phase angles uniformly distributed between 0 and 2π; $\omega_i = i\Delta\omega$ is the discrete frequency and $\Delta\omega = \omega_{cut}/\bar{d}$, in which $\omega_{cut} = 30\pi$ is the cut-off frequency.

The limit-state function is expressed as in Eq. (17), with the top story displacement being the response of interest and a threshold $\lambda = 0.229$. Results, accompanied by the ASTPA parameters, are shown in Table 3(a) based on sampling in the standard normal space. As seen, our ASTPA approach considerably outperforms SuS, with $n_s = 4,000$, in this challenging example, while QNp-HMCMC shows improved computational efficiency compared to the original HMCMC sampler.

The first-passage probability is also directly computed in the non-Gaussian space in this example. Given that the random variables involved in the SRM are uniformly distributed with $\boldsymbol{\theta} \in$

$[0, 2\pi]$, they are first transformed to the unconstrained space for the HMCMC-based sampling, see (Papakonstantinou et al., 2022) for transformation details. It should be noted that the stiffness Gaussian random variables have been transformed to the standard normal space in both cases.

Table 3(b) displays the obtained results based on the non-Gaussian space sampling. Compared to the typical HMCMC method, and noting also the difference in the number of model calls between the two HMCMC approaches, this example further supports the results in (Papakonstantinou et al., 2023), and confirms that the application of QNp-HMCMC in high-dimensional challenging problems is in general very attractive and most appropriate. For SuS in this non-Gaussian space, we could not achieve any competitive and meaningful results. Comparing Tables 3(b) and 3(a), we also note that the results based on the Gaussian space sampling are overall better than those in the non-Gaussian one, an effect that could be perhaps expected due to the favorable sampling attributes of the normal space.

6. CONCLUSIONS

The ASTPA (Approximate Sampling Target with Post-processing Adjustment) framework for precisely estimating rare event probabilities is successfully applied to complex first-passage dynamic problems. ASTPA can provide accurate, unbiased estimations of rare events probabilities with an efficient number of limit-state function evaluations. The basic idea of ASTPA is to construct a relevant target distribution by weighting the high-dimensional random variable space through a one-dimensional likelihood model, using the limit-state function. To sample from this target distribution, we utilize here gradient-based HMCMC schemes, including our newly developed efficient Quasi-Newton mass preconditioned HMCMC algorithm (QNp-HMCMC). In the absence of analytical gradients for the examined problems, then the presented sampling schemes would require numerical gradient estimations and would not probably be computationally competitive anymore. The performance of the proposed methodology is examined and compared very successfully herein against Sub-

set Simulation in challenging, high-dimensional, nonlinear, stochastic dynamic problems, involving model uncertainties and stochastic processes expressed through white noise, Karhunen-Loève (K-L) expansion, and the Spectral Representation Method, with implementation and sampling in both non-Gaussian and standard Gaussian spaces.

7. REFERENCES

Andrieu-Renaud, C., Sudret, B., and Lemaire, M. (2004). "The PHI2 method: A way to compute time-variant reliability." *Reliability Engineering & System Safety*, 84(1), 75–86.

Au, S.-K. and Beck, J. L. (2001). "Estimation of small failure probabilities in high dimensions by Subset Simulation." *Probabilistic Engineering Mechanics*, **16**(4), 263–277.

Biondini, G. (2015). "An introduction to rare event simulation and importance sampling." *Handbook of Statistics*, Vol. 33, Elsevier, 29–68.

Neal, R. M. (2011). "MCMC using Hamiltonian dynamics." *Handbook of Markov Chain Monte Carlo*, **2**(11), 113–162.

Papaioannou, I., Geyer, S., and Straub, D. (2019). "Improved cross entropy-based importance sampling with a flexible mixture model." *Reliability Engineering & System Safety*, 191, 106564.

Papakonstantinou, K. G., Nikbakht, H., and Eshra, E. (2022). "Quasi-Newton Hamiltonian MCMC sampling for reliability estimation in high-dimensional non-Gaussian spaces." *The 13th International Conference on Structural Safety and Reliability (ICOSSAR)*.

Papakonstantinou, K. G., Nikbakht, H., and Eshra, E. (2023). "Hamiltonian MCMC methods for estimating rare events probabilities in high-dimensional problems." *Probabilistic Engineering Mechanics (under review), arXiv preprint arXiv:2007.00180*.

Song, J. and Der Kiureghian, A. (2006). "Joint first-passage probability and reliability of systems under stochastic excitation." *Journal of Engineering Mechanics*, 132(1), 65–77.

Zhang, D., Han, X., Jiang, C., Liu, J., and Li, Q. (2017). "Time-dependent reliability analysis through response surface method." *Journal of Mechanical Design*, 139(4), 041404.